Sociedade Brasileira de Automática (SBA)
XXIV Congresso Brasileiro de Automática - CBA 2022, 16 a 19 de outubro de 2022

Optimal Tuning of FOPID Controller for a MIMO Aircraft Model Using Swarm Intelligence

Odilon L. C. Mendes * **Guilherme A. Barreto** **
Mauricio A. V. Morales ***

* *Instituto Tecnológico de Aeronáutica, SP, Brazil, (e-mail: odilonolcm@ita.br).*
** *Departamento de Engenharia de Teleinformática, Universidade Federal do Ceará, CE, (e-mail: gbarreto@ufc.br)*
*** *Instituto Tecnológico de Aeronáutica, SP, Brazil, (e-mail: morales@ita.br)*

Abstract: Control systems of aircraft dynamics focus on choosing configurations that meet certain criteria related to speed response, damping ratio, error in steady state, among others. Aeronautical engineering applications have safety requirements, and in this respect, the use of optimization algorithms assist in the ability to develop models of increasing complexity. Therefore, the main objective of this work is to develop a methodology for optimal tuning of fractional order proportional integral derivative (FOPID) controller based on particle swarm optimization (PSO) for multiple input multiple output (MIMO) aircraft model. This work can contribute to the aeronautical performance through the development of simulations seeking the best parameters from the controller, allowing flight conditions according to pre-established requirements. Three stochastic optimization algorithms were studied: global random search (GRS), local random search (LRS) and PSO. The PSO delivered the best results. Different performance indices based on the integral of error were used as objective functions. The ITAE (integral of time multiplied by the absolute error) index was chosen for presenting the best performance. It was necessary to limit the input values of the models, taking into account the limitation of the integrator term of the controller based on the anti-windup (AW) technique. Based on the prerequisites for the aircraft, the performance metrics achieved results considered adequate to the challeging demands of the task.

Keywords: Control Systems; Swarm Intelligence; Aircraft Dynamics; Particle Swarm Optimization; Fractional Order PID

1. INTRODUCTION

Aircraft are primarily responsible for the rapid transport of passengers and cargo over short or long distances and are fundamental to the global economy. The design of an aircraft depends on the automatic control system that monitors and controls its subsystems. The development of these systems played an important role in the growth of civil and military aviation. Problems related to stability and control are studied in order to guarantee greater safety and comfort for the crew and passengers. Small variations in the equilibrium condition are enough to cause changes in the stable and maneuvering behavior of an aircraft (Cook, 2012). Control systems ensure the change of a flight condition to another quickly and smoothly, the aircraft remaining stable.

The dynamic response characteristics of an aircraft vary nonlinearly across the flight envelope. Traditionally, flight control systems have used linearized mathematical models in various flight conditions, with the controller parameters varying with a variation of flight operating states. During the past few decades, control techniques have experienced many advances. In spite of these advances, an example is the PID controller. It is widely used due to its simple structure and acceptable performance in a wide range of operating conditions (Gaing, 2004). A new possibility of extending the standard PID was introduced relatively recent, being called fractional order PID (FOPID). As a generalization of the traditional PID, the FOPID controller aims at dealing with plants of more complex dynamics, providing a more adequate control system (Shah and Agashe, 2016; Podlubny, 1994). The fractional order of the integral and derivative terms adds extra degrees of freedom to the control task, since it has two additional tunable parameters, keeping the same structure as the PID controller (Grandi, 2018).

Despite the increasing interest of the control community for the properties of the FOPID controller, some issues still remain open, in particular those related with parameter tuning. There are some heuristic methods to tune FOPID controllers, although it is still difficult to determine the optimal parameters (Krohling and Rey, 2001). Most PID tuning approaches are aimed at controlling SISO systems, as example the linear programming based methods (Euzébio et al., 2020). Few works are focused on tuning controllers for MIMO systems, some methods include, marine predators algorithm (Yan Lieven Souza Lúcio and dos

Santos Coelho., 2021), artificial neural networks (Hosseini et al., 2020), neuro-fuzzy (Shi et al., 2020), and swarm intelligence-based algorithms (Chang, 2007).

PSO is the state of the art in metaheuristic optimization algorithms. It was developed through the simulation of a simplified social system, and has been used for global optimization of continuous nonlinear problems (Kennedy and Eberhart, 1995). PSO is a population-based algorithm and the search for the optimal solution is done in parallel directions, instead of a single one.

In practical control systems, aeronautical engineering applications have increasingly restrictive safety requirements, and in this respect, the use of optimization algorithms assist in the development of suitable control systems. Therefore, the main objective of this work is to develop a method for optimal tuning of controller in a MIMO aircraft system based on a set of techniques involving FOPID controller, PSO algorithm and AW back-calculation strategy.

2. THE AIRCRAFT MODEL

Aircraft modeling is based on two aspects: the estimation of aerodynamic parameters and the development of differential equations that describe the aircraft movement. It is through the differential equations that the estimated outputs of the model can be obtained. According to the aerodynamics, propulsive and atmospheric models and the adopted body coordinate system, the twelve equations that represent the translational and rotational dynamics and kinematics of an aircraft can be determined. The work of Stevens et al. (2015) is a suitable reference for more details about aircraft modeling.

The model used is a lateral-directional control augmentation system. The equations are decoupled and linearized around the equilibrium point, allowing the derivation of second order model in the state space and transfer function for movements. It is a MIMO system for the F-16 jet fighter. The reference for this model is the book Aircraft Control and Simulation, example of Lateral-Directional Stability Augmentation (Yaw Damper) (Stevens et al., 2015).

The F-16 model does not include flaps and landing gear, so the design is illustrated on a low-speed, and low-altitude flight condition. The control augmentation systems (CAS) state equations are linearized and the coefficient matrices are represented by

$$\dot{x} = Ax + Bu \tag{1}$$

$$x = Cy \tag{2}$$

$$\dot{x} = \begin{bmatrix} \dot{\beta} \\ \dot{\phi} \\ \dot{\psi} \\ \dot{p} \\ \dot{r} \end{bmatrix}, u = \begin{bmatrix} \delta_a \\ \delta_r \end{bmatrix}, y = \begin{bmatrix} \beta \\ \phi \end{bmatrix} \tag{3}$$

$$A = \begin{bmatrix} -0.1315 & 0.14858 & 0 & 0.32434 & -0.93964 \\ 0 & 0 & 0 & 1 & 0.33976 \\ 0 & 0 & 0 & 0 & 1.0561 \\ -10.614 & 0 & 0 & -1.1793 & 1.0023 \\ 0.99655 & 0 & 0 & -0.0018174 & -0.25855 \end{bmatrix} \tag{4}$$

$$B = \begin{bmatrix} 0.00012049 & 0.00032897 \\ 0 & 0 \\ 0 & 0 \\ -0.1031578 & 0.020987 \\ -0.002133 & -0.010715 \end{bmatrix} \tag{5}$$

$$C = \begin{bmatrix} 57.29578 & 0 & 0 & 0 & 0 \\ 0 & 57.29578 & 0 & 0 & 0 \end{bmatrix} \tag{6}$$

where the state variables are the sideslip angle (β), roll angle (ϕ), yaw angle (ψ), roll rate (p) and yaw rate (r), the input variables are aileron angle (δ_a) and rudder angle (δ_r), and roll rate (p) and yaw rate (r) are the output variables.

3. THE CONTROL SYSTEM

The PID is one of the most used controllers in the industry (Koivo and Tanttu, 1991). One of the reasons for the success of this controller is its mathematical simplicity, which can be applied to an extensive number of dynamic processes with a satisfactory performance. The most common form of the PID controller equation in the continuous time domain is given by

$$u(t) = K_p e(t) + K_i \int_0^t e(t)dt + K_d \frac{de(t)}{dt} \tag{7}$$

in which $u(t) \in R$ is the control action, K_p, K_i and K_d are the parameters for each controller term (gains), and $e(t) = r(t) - y(t)$ is the error signal at the current time ($e(t) \in R$), that is, the difference between the reference signal (or setpoint) $r(t) \in R$ and the system output signal (or controlled output) $y(t) \in R$.

The fractional order PID controller (FOPID) is an extension of the PID controller. The FOPID has drawn attention in recent years due to its potential to offer extra degrees of freedom to the modeling task while maintaining the baseline simplicity of a PID controller (Grandi, 2018).

The math used by this controller is based on fractional calculus, or non-integer order calculus. A characteristic of fractional calculus is that it does not depend only on the local properties of the function, it considers the history and the non-local distributed effects (Das, 2008). The FOPID controller is generically symbolized as $PI^{\lambda}D^{\mu}$ and described mathematically by the following differential equation:

$$u(t) = K_p e(t) + K_i D^{-\lambda} e(t) + K_d D^{\mu} e(t) \tag{8}$$

in which λ is the order of the integral, μ is the order of the derivative, and D is the derivative operator. The parameters λ and μ are positive or null real numbers.

The Newtonian derivative is the basis for understanding fractional order differential equations. Taking this into account, three methods stand out of many definitions for the fractional derivative, that are the Grunwald-Letnikov, Riemann-Liouville and Caputo. These definitions can often be found in the literature related to the FOPID controller (Das, 2008; Chopade et al., 2016). The definition of Grunwald-Letnikov, used in this work, for fractional order derivative/integral is given by

$$ {}_{t_0}\mathrm{D}_t^{\alpha} f(t) = \lim_{h\to 0} \frac{1}{h^{\alpha}} \sum_{j=0}^{[t-t_0/h]} (-1)^j \binom{\alpha}{j} f(t-jh) \tag{9} $$

in which α is the order of the operator, determining whether to perform an integration ($\alpha < 0$) or a differentiation ($\alpha > 0$). The lower and upper limits for the operator are defined by t_0 and t, respectively. The upper limit of the summation, defined as $[(t - t_0/h)]$, is the integer part of the expression. It is observed that the differential and integral operators are used into the fundamental operator $D^{\alpha} f(t)$ represented by

$$ D^{\alpha} f(t) = \left\{ \begin{array}{lcc} {}_{t_0}\mathrm{D}_t^{\alpha} f(t), & & -1 < \alpha < 1 \\ \dfrac{df(t)}{dt}, & \rightarrow & \alpha = 1 \\ \displaystyle\int f(t)dt, & & \alpha = -1 \end{array} \right| \tag{10} $$

in which α is the parameter that determines the type of operation that will be performed.

4. PERFORMANCE INDICES

In the search for optimal solutions, a common and effective approach is to search for controller parameters that optimize a performance index, such as an error function between the desired and obtained response by a system (Boudjehem and Boudjehem, 2016).

A function of the response error of a closed loop system is, perhaps, the main measure for an objective function in controller optimization. The combination of the error accumulated with the time can be used in different possibilities (Dorf and Bishop, 2001), and some of them can be seen below.

Integral Squared Error (ISE):

$$ ISE = \int_0^T e^2(t)dt \tag{11} $$

Integral Absolute Error (IAE):

$$ IAE = \int_0^T |e(t)|\, dt \tag{12} $$

Integral Time Squared Error (ITSE):

$$ ITSE = \int_0^T te^2(t)dt \tag{13} $$

Integral Time Absolute Error (ITAE):

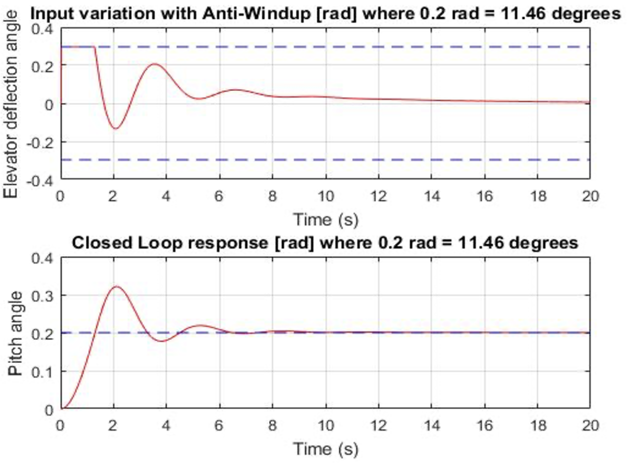

Figure 1. Windup phenomenon, where the output is the elevator deflection and the control signal is the pitch angle. It is possible to observe the saturation for almost 2 seconds and the output response with a huge overshoot and oscillating. The reference signal is 0 rad for the elevator deflection angle, and 0.2 rad for the pitch angle.

$$ ITAE = \int_0^T t\, |e(t)|\, dt \tag{14} $$

5. ANTI-WINDUP SYSTEM

In practical control systems, it may happen the control variable to reach the actuator limits. When this happens the feedback loop is broken and the system runs as an open loop because the actuator will remain at its limit independently of the process output. If a controller with integrating action is used, the error will continue to be accumulated. This means that the integral term may become very large or, in layperson words, it winds up. The consequence is that any controller with integral action could yield large transients when the actuator saturates. The windup phenomenon is illustrated in Figure 1.

The output remains saturated because of the large value of the integral term. It does not leave the saturation limit until the error has been negative for a sufficiently time to let the integral part comes down to a small level. The effect is a large overshoot and a damped oscillation. The back-calculation method (Kavyashree et al., 2022; Fertik and Ross, 1967) can be used to avoid windup phenomenon.

If the output saturates, the integral term is recomputed and its new value yields an output at the saturation limit. It is advantageous not to reset the integrator instantaneously but dynamically with a time constant T_t. In Figure 2, it is shown a block diagram of a PID controller with anti-windup (AW) based on back-calculation.

6. MIMO FOPID TUNING BY PSO ALGORITHM

Optimization algorithms, such as metaheuristic optimization, are an option for adjusting parameters of complex systems. The GRS and LRS algorithms have one candidate solution being evaluated per iteration (Horst and Pardalos, 2013; Horst and Tuy, 2013; Boender and Romeijn, 1995),

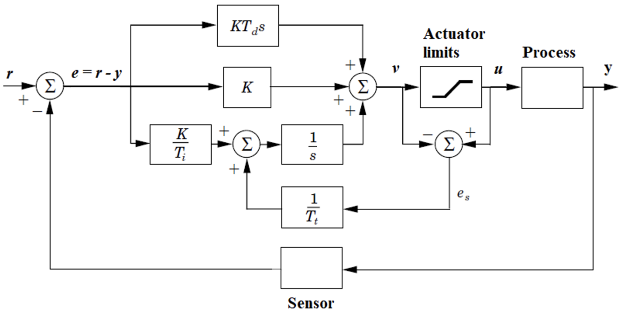

Figure 2. Block diagram of a PID controller with AW based on back-calculation.

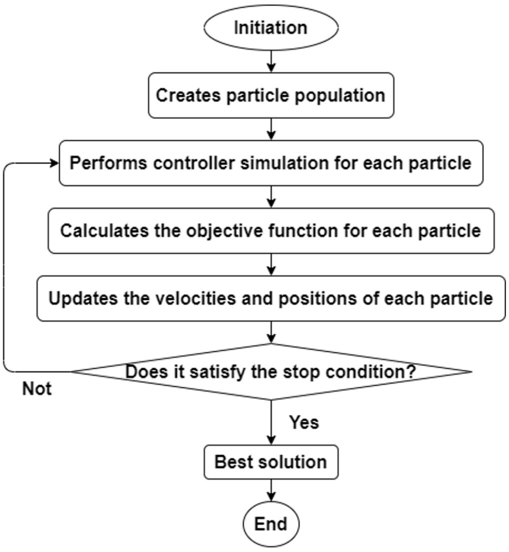
Initiation
Creates particle population
Performs controller simulation for each particle
Calculates the objective function for each particle
Updates the velocities and positions of each particle
Does it satisfy the stop condition?
Not
Yes
Best solution
End

Figure 3. Flowchart of a swarm intelligence algorithm.

while the PSO algorithm has many candidate solutions being evaluated per iteration. In Figure 3, it is shown the flowchart of a general swarm intelligence algorithm.

The PSO is inspired by social behavior and the self-organization of groups of migratory birds and schools of fish (Shi and Eberhart, 1999). The solutions are represented by particles with specific position and velocity forming a swarm in a space of possible solutions (Mendes et al., 2004). The variables that make up the solution are grouped into a vector formed by real numbers. There is an exchange of global and local information, that is, there is a balance between exploration and exploitation (Mattos et al., 2014). The step-by-step for PSO approach can be seen below.

(1) Initialize all x_i and v_i with random values and p_i and p_g with null values.
(2) Calculate the value of the objective function $f(x)$ for each particle. The vector p_i of each particle receives x_i, while vector p_g receives the position corresponding to the best objective function of the swarm.
(3) Update v_i and x_i applying the particle update rules (Equations (19) and (20)).
(4) If x_i exceeds the searching space limits it receives the values of the last p_i.
(5) Evaluate the objective function $f(x)$ for all particles.
(6) Update p_i if the i-th particle current position corresponds to a better cost function.
(7) Update p_g if a better global solution is found.
(8) Repeat the process from Step 3 until a stop condition is found.

where x_i is the d-dimensional position vector of the i-th particle, v_i is the d-dimensional velocity vector of the i-th particle, p_i best solution found by the i-th particle, p_g is the best global solution found by the swarm, w is the inertia parameter, c_1, c_2 are the accelerating coefficients, and r_1, r_2 are the pseudo-random numbers uniformly distributed between 0 and 1.

In Step 3, x_i and v_i are updated by applying the particle update rules. The velocity of a particle is updated by

$$v_i(t+1) = v_i(t) + \Delta v_i(t) \tag{15}$$

The $\Delta v_i(t)$ consists of two parts (local and global), and it is represented by

$$\Delta v_i(t) = \Delta v_i^{(1)}(t) + \Delta v_i^{(2)}(t) \tag{16}$$

The topology $\Delta v_i^{(1)}(t)$ (local part) represents the difference between the best position of the i-th particle p_i and its current position x_i, which is represented by

$$\Delta v_i^{(1)}(t) = c_1 r_1 (p_i - x_i(t)). \tag{17}$$

In the global part of Equation (16), $\Delta v_i^{(2)}(t)$ represents the difference between the best global position of the particle swarm p_g and the current position of the i-th particle x_i, which is represented by

$$\Delta v_i^{(2)}(t) = c_2 r_2 (p_g - x_i(t)). \tag{18}$$

The terms r_1 and r_2 help in the search randomness while the terms c_1 and c_2 command the acceleration of the coefficients. Therefore, the Equation (15) can be described by

$$v_i(t+1) = w v_i(t) + c_1 r_1 (p_i - x_i(t)) + c_2 r_2 (p_g - x_i(t)). \tag{19}$$

The term w is an inertia parameter that acts against sudden movements. It provides stability to the algorithm. The position of a particle is updated by

$$x_i(t+1) = x_i(t) + v_i(t+1) \tag{20}$$

Thereby, optimization through the PSO algorithm can be understood by Equations (19) and (20). The optimal solution or solutions are dependent on the objective function which is a fundamental part of the problem design.

7. METHODOLOGY

The first parameters are those related to the discretization of the model, they are: $h = 0.01$ s; $T_{sim} = 10$ to 20 s; $t = (T_{sim}/h) + 1$; L = size of vector t. In which h is the discretization step, T_{sim} is the simulation time, t counts the sampling instants, L serves to know the size of the desired, or reference, output vector.

For the FOPID controller, the gains K_p, K_i and K_d are chosen within the range between -10 and 10. The initial exponents λ and μ start with the value of 1, which corresponds to a common PID, as the exponents go through the search space, which varies between 0 and 1, the controller stops being PID and become FOPID. The parameter K_0 is set to the value 1 that means linear fractional controller.

The execution of PSO can be seen in details through the following steps:

(1) Initialize all x_i and v_i with random values and p_i and p_g with null values.
(2) Calculate the value of the objective function $f(x)$ for each particle. The vector p_i of each particle receives x_i, while vector p_g receives the position corresponding to the best objective function of the swarm.
(3) The algorithm starts through the use of the initial parameters M (population size, or vector size) = 50, $c_1 = c_2 = 2$ and, r_1, r_2 and $w = 0.1$;
(4) Define all variables as vectors of size M;
(5) The interval constraints for the search variables (controller parameters) are specified in Table 1;
(6) The initial random parameters are set as the best current parameters ($K_{p(best)}$, $K_{i(best)}$, $K_{d(best)}$, $\lambda_{(best)}$, $\mu_{(best)}$) resulting in a best solution ($J_{(best)}$);
(7) Initialization of v_i with null values, x_i with random values, p_i with the best current parameters ($K_{p(best)}$, $K_{i(best)}$, $K_{d(best)}$, $\lambda_{(best)}$, $\mu_{(best)}$), and p_g with the best current parameters of the population M;
(8) Calculate the value of the objective function $J_{(cand)}$ for each particle. The vector p_i of each particle receives $K_{p(cand)}$, $K_{i(cand)}$, $K_{d(cand)}$, $\lambda_{(cand)}$, $\mu_{(cand)}$) while vector p_g receives the position corresponding to the best objective function of the swarm;
(9) Update v_i and x_i applying the particle update rules of Equations (19) and (20);
(10) Evaluate the objective function $J_{(cand)}$ for all particles;
(11) Update p_i if the current position of the i-th particle corresponds to a better objective function, and update p_g if a better global solution is found;
(12) Update the inertial parameter (w) for each iteration N_i:

$$w = r_2 + \frac{(r_1 - r_2)(N_i - t)}{N_i - 1} \tag{21}$$

(13) The process is repeated for 500 iterations (N_i) in 40 epochs (z);
(14) At the end of the process it will have 40 best different solutions ($J_{(best)}$) with their respective parameters ($K_{p(best)}$, $K_{i(best)}$, $K_{d(best)}$, $\lambda_{(best)}$, $\mu_{(best)}$);
(15) From the 40 best different solutions, the one with the minimum value will be chosen.

Table 1. Limits of the control signals (actuators) considering real-world safety constraints.

Control surface	Displacement range	Displacement rate
Rudder	[-30, +30] deg	120 deg/s
Aileron	[-21.5, +21.5] deg	80 deg/s

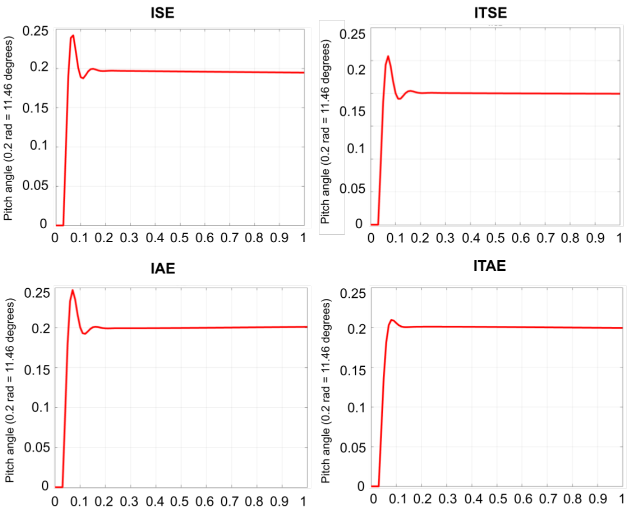

Figure 4. Closed-loop steps response for the FOPID controller tuned by the PSO algorithm.

8. RESULTS AND DISCUSSIONS

The results of preliminary experiments were used to define the components of the methodology for tuning the parameters of the FOPID controller, that is, which optimization algorithm and which performance index will be used. The proposed methodology was analyzed in 4 controller configurations: PID, PID+AW, FOPID, and FOPID+AW. The results were discussed based on the performance results for each situation.

8.1 Effect of the Performance Indices

In Figure 4 is shown different responses for ISE, ITSE, IAE and ITAE indices using PSO. The chosen methods were the ITAE performance index and the PSO search algorithm, as they provided the lower overshoot and the lower accomodation time in steady state. The number of iterations, realizations, and population size will be 100, 40 and 50, respectively. The reference signal is 0.2.

8.2 Anti-Windup Implementation

It is necessary to limit the input values of the model for safety reasons, taking into account the limitation of the integrator term of the controller. For this, the anti-windup system is used. The results of the input and output values are satisfactory, within the design prerequisites, as can be seen in Figure 5.

8.3 Lateral-Directional Control Augmentation System

The desired response in steady state for the regulator sideslip angle (β) is 0 degrees and the desired step response for bank angle (ϕ) is 15 degrees. These values are within the parameter limits for both outputs.

PID Control Results In Table 2 are shown the optimal values of the PID gains associated with the best value of the ITAE index after 40 independent realizations of the PSO-based tuning methodology.

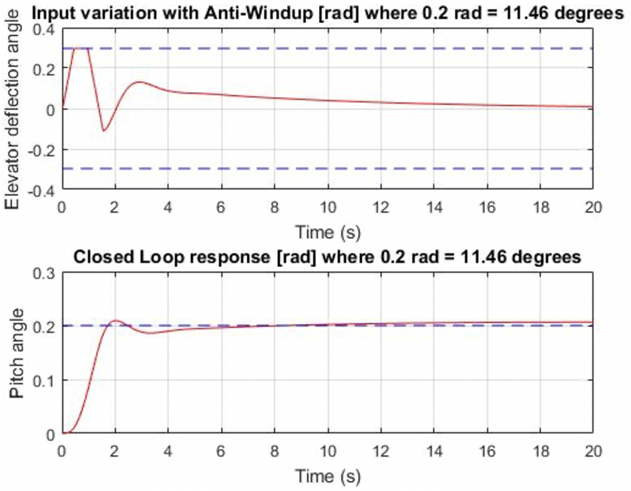

Figure 5. Input (top) and output (bottom) responses with saturation constraints on the control signal and applying the anti-windup system. The reference signal is 0 rad for the elevator deflection angle, and 0.2 rad for the pitch angle.

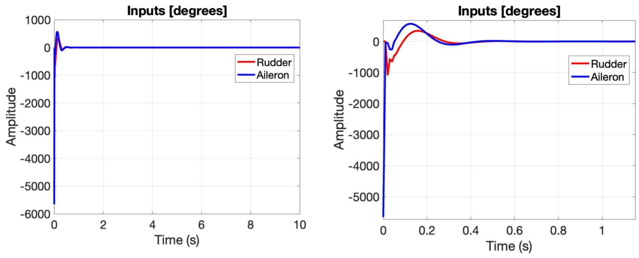

Figure 6. Control signals for the the PID control.

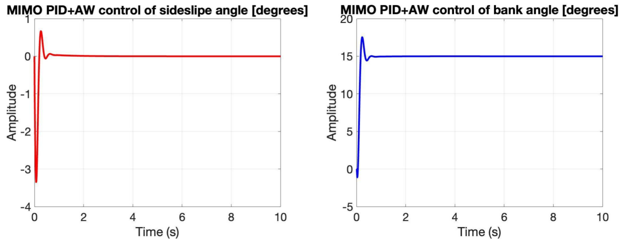

Figure 7. Output responses for the the PID control.

The input signals are shown in Figure 6. The output responses are shown in Figure 7. The reference signal is 0 degrees for the sideslip angle, and 15 degrees for the bank angle. The performance results for the system output are shown in Table 3.

Table 2. Optimal parameters of MIMO PID controller tuned by PSO.

K_{p1}, K_{i1}, K_{d1}	K_{p2}, K_{i2}, K_{d2}	ITAE
-9.0056, 1.1215, -9.9991	-2.9913, -0.5786, -3.7387	39.4095

Table 3. Performance of the PID controller.

Output	Rise	Peak	Overshoot	Setlling	SSE
β	-	0.32 s	334.83 %	0.36 s	0.0144 %
ϕ	0.18 s	0.24 s	16.94 %	0.28 s	0.003 %

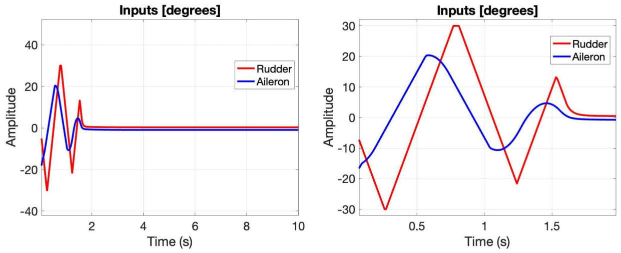

Figure 8. Control signals for the the PID+AW control.

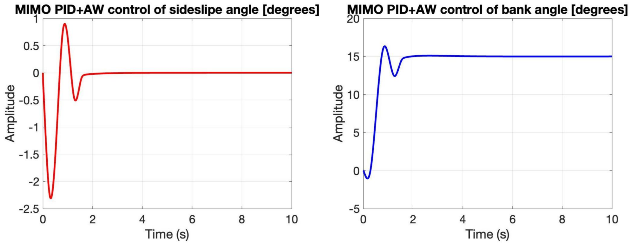

Figure 9. Output responses for the PID+AW control.

The closed loop MIMO system using PID controller is stable by observing the steady-state errors of the output responses. These errors are null or constant with nearly null values. The performance results can be considered adequate, however, it is necessary to take into account the limitations of the control signals. In Figure 6 is possible to observe that the rudder actuator reaches close to 1000 degrees in milliseconds, and the aileron actuator reaches close to 6000 degrees in milliseconds, an infeasible situation in real-world scenario. The processing time after 40 independent realizations of the PSO-based tuning was 6.50 minutes.

PID+AW Control Results In Table 4 are shown the optimal values of the PID+AW gains associated with the best value of the ITAE index after 40 independent realizations of the PSO-based tuning methodology.

Table 4. Optimal parameters of the MIMO PID with AW tuned by PSO.

K_{p1}, K_{i1}, K_{d1}	K_{p2}, K_{i2}, K_{d2}	ITAE
-2.2674, 0.3435, -7.0244	-0.6166, -0.1097, -0.6312	497.7268

The input signals are shown in Figure 8. The output responses are shown in Figure 9. The reference signal is 0 degrees for the sideslip angle, and 15 degrees for the bank angle. The performance results for the system output are shown in Table 5.

Table 5. Performance of the PID+AW.

Output	Rise	Peak	Overshoot	Setlling	SSE
β	-	0.92 s	230.9408 %	1.54 s	0.0892 %
ϕ	0.74 s	0.87 s	8.959 %	1.41 s	0.0065 %

The performance results can be considered satisfactory even with the limitations imposed on the control signals. In Figure 8 is possible to observe that the control signal is within the specified limits of the actuator. The processing time after 40 independent realizations of the PSO-based tuning was 36.21 minutes.

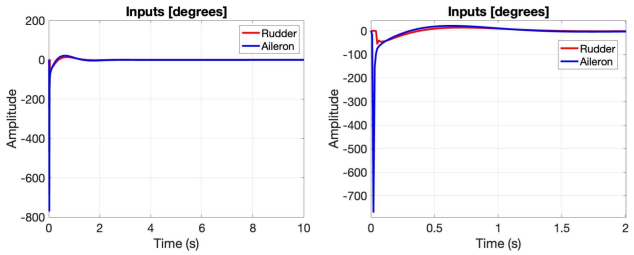

Figure 10. Control signals for the the FOPID control.

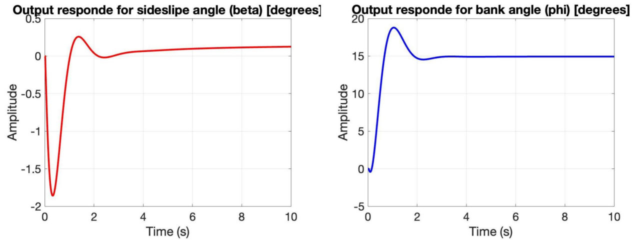

Figure 11. Output responses for the the FOPID control.

FOPID Control Results In Table 6 are shown the optimal values of the FOPID gains associated with the best value of the ITAE index after 40 independent realizations of the PSO-based tuning methodology.

Table 6. Optimal parameters of MIMO FOPID tuned by PSO.

K_{p1}, K_{i1}, K_{d1}, λ_1, μ_1	K_{p2}, K_{i2}, K_{d2}, λ_2, μ_2	ITAE
-0.99 -8.41, 4.46, 0.44, 0.96	-1.08, 2.43, 1.24, 0.61, 0.82	2001.46

The input signals are shown in Figure 10. The output responses are shown in Figure 11. The reference signal is 0 degrees for the sideslip angle, and 15 degrees for the bank angle. The performance results for the system output are shown in Table 7.

Table 7. Performance of the FOPID control.

Output	Rise	Peak	Overshoot	Setlling	SSE
β	-	1.34 s	185.8715 %	1.86 s	12.4236 %
ϕ	0.68 s	1.06 s	25.2284 %	1.52 s	1.52 %

The performance results can also be considered adequate, however, it is necessary to take into account the limitations of the control signals. In Figure 10 is possible to observe that the rudder actuator reaches close to 1800 degrees in milliseconds, and the aileron actuator reaches close to 150 degrees in milliseconds, an infeasible situation in real-world scenario. The processing time after 40 independent realizations of the PSO-based tuning was 182.40 minutes (3.04 hours).

FOPID+AW Control Results In Table 8 are shown the optimal values of the FOPID+AW gains associated with the best value of the ITAE index after 40 independent realizations of the PSO-based tuning methodology.

Table 8. Optimal parameters of the MIMO FOPID with AW tuned by PSO.

K_{p1}, K_{i1}, K_{d1}, λ_1, μ_1	K_{p2}, K_{i2}, K_{d2}, λ_2, μ_2	ITAE
-1.78 -9.43, 9.98, 0.04, 0.97	-3.12, 8.13, 8.7, 0.16, 1	6087.3

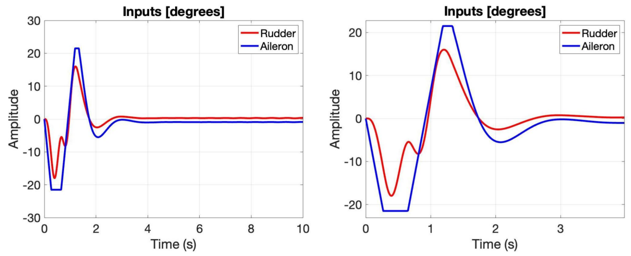

Figure 12. Control signals for the the FOPID+AW control.

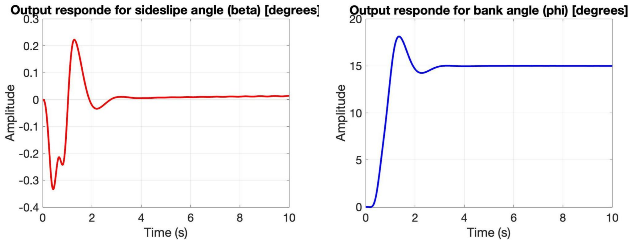

Figure 13. Output responses for the the FOPID+AW control.

The input signals are shown in Figure 12. The output responses are shown in Figure 13.The reference signal is 0 degrees for the sideslip angle, and 15 degrees for the bank angle. The performance results for the system output are shown in Table 9.

Table 9. Performance of the FOPID+AW control.

Output	Rise	Peak	Overshoot	Setlling	SSE
β	-	1.26 s	33.3454 %	1.61 s	1.3805 %
ϕ	1.06 s	1.36 s	20.8131 %	1.66 s	0.0218 %

The performance results can be considered satisfactory even with the limitations imposed on the control signals. In Figure 12 is possible to observe that the control signal is within the specified limits of the actuator. The processing time after 40 independent realizations of the PSO-based tuning was 862.23 minutes (14.37 hours).

Evaluation of the Control Strategies The results for the four different approaches can be considered satisfactory, as they are within the specified prerequisites. Comparing PID, PID+AW, FOPID and FOPID+AW controllers, it is observed that the FOPID and FOPID+AW results are better only in terms of the overshoot. The PID and PID+AW performed better in terms of rise time, peak time, settling time and steady state error. Therefore, taking into account the importance of overshoot for different control situations and the small difference between the results of rise time, peak time, settling time and steady state error, we can conclude that the FOPID controller is a more appropriate choice.

9. CONCLUSIONS

The main objective of this work was the development of a methodology for optimal tuning of controllers in a MIMO aircraft model based on a set of techniques involving both, PID and FOPID controllers, PSO algorithm and anti-windup back-calculation strategy. In addition, other objectives were also pursued: a comparison of the performance of the PSO algorithm with alternative stochastic optimization algorithms, the GRS and the LRS; an evaluation of the influence of different performance indices, such as ISE, IAE, ITSE and ITAE, in the performance of the optimal control system; and the application of an anti-windup strategy to limit control signals according to the real-world constraints of aircraft's actuators (ailerons, rudder) in order to guarantee the most possible realistic simulation.

There is a limited amount of research on control systems involving FOPID controllers, and when incorporated into MIMO system using anti-windup strategy, no work was observed in the area of aerodynamic models developing something similar. The concern with the simulation being the closest to reality added yet another weight factor, the use of the anti-windup strategy to limit the control signals as they occur in real practices. It can be concluded that the implementation of this set of techniques, which are at the forefront of science, provide a differential in the implemented methodology.

10. ACKNOWLEDGMENTS

This research was partly funded by CAPES (finance code 001), FUNCAP and CNPq (grant 309379/2019-9).

REFERENCES

Boender, C.G.E. and Romeijn, H.E. (1995). Stochastic methods. in: R. HORST; P. M. PARDALOS (eds.), handbook of global optimization. *Boston, MA: Springer*, 829–869.

Boudjehem, B. and Boudjehem, D. (2016). Fractional PID controller design based on minimizing performance indices. *IFAC-PapersOnLine*, 49(9), 164–168.

Chang, W.D. (2007). A multi-crossover genetic approach to multivariable PID controllers tuning. *Expert systems with applications*, 33(3), 620–626.

Chopade, A.S., Khubalkar, S.W., Junghare, A.S., Aware, M.V., and Das, S. (2016). Design and implementation of digital fractional order PID controller using optimal pole-zero approximation method for magnetic levitation system. *IEEE/CAA Journal of Automatica Sinica*, 5(5), 977–989.

Cook, M.V. (2012). *Flight dynamics principles: a linear systems approach to aircraft stability and control.* Butterworth-Heinemann.

Das, S. (2008). Fractional calculus for system identification and controls.

Dorf, R.C. and Bishop, R.H. (2001). *Modern Control Systems: Solutions Manual*, volume 12. Prentice Hall.

Euzébio, T.A., Yamashita, A.S., Pinto, T.V., and Barros, P.R. (2020). Siso approaches for linear programming based methods for tuning decentralized pid controllers. *Journal of Process Control*, 94, 75–96.

Fertik, H.A. and Ross, C.W. (1967). Direct digital control algorithm with anti-windup feature. *ISA Transactions*, 6(4), 317–.

Gaing, Z.L. (2004). A particle swarm optimization approach for optimum design of PID controller in AVR system. *IEEE transactions on energy conversion*, 19(2), 384–391.

Grandi, G.L. (2018). Comparação entre controladores PID e FOPID baseada em novo método de ajuste.

Horst, R. and Pardalos, P.M. (2013). Handbook of global optimization. *Boca Raton: Springer Science Business Media.*

Horst, R. and Tuy, H. (2013). Global optimization: Deterministic approaches. *Springer Science Business Media.*

Hosseini, S.A., Shirani, A.S., Lotfi, M., and Menhaj, M.B. (2020). Design and application of supervisory control based on neural network PID controllers for pressurizer system. *Progress in Nuclear Energy*, 130, 103570.

Kavyashree, B., Patil, S., and Rao, V.S. (2022). Observer-based anti-windup robust PID controller for performance enhancement of damped outrigger structure. *Innovative Infrastructure Solutions*, 7(3), 1–16.

Kennedy, J. and Eberhart, R. (1995). Particle swarm optimization. In *Proceedings of ICNN'95-international conference on neural networks*, volume 4, 1942–1948. IEEE.

Koivo, H. and Tanttu, J. (1991). Tuning of PID conrollers: Survey of SISO and MIMO techniques. In *Intelligent tuning and adaptive control*, 75–80. Elsevier.

Krohling, R.A. and Rey, J.P. (2001). Design of optimal disturbance rejection PID controllers using genetic algorithms. *IEEE Transactions on Evolutionary computation*, 5(1), 78–82.

Mattos, C.L., Barreto, G.A., and Cavalcanti, F.R. (2014). An improved hybrid particle swarm optimization algorithm applied to economic modeling of radio resource allocation. *Electronic Commerce Research*, 14(1), 51–70.

Mendes, R., Kennedy, J., and Neves, J. (2004). The fully informed particle swarm: simpler, maybe better. *IEEE transactions on evolutionary computation*, 8(3), 204–210.

Podlubny, I. (1994). Fractional-order systems and fractional-order controllers. *Institute of Experimental Physics, Slovak Academy of Sciences, Kosice*, 12(3), 1–18.

Shah, P. and Agashe, S. (2016). Review of fractional PID controller. *Mechatronics*, 38, 29–41.

Shi, Q., Lam, H.K., Xuan, C., and Chen, M. (2020). Adaptive neuro-fuzzy PID controller based on twin delayed deep deterministic policy gradient algorithm. *Neurocomputing*, 402, 183–194.

Shi, Y. and Eberhart, R.C. (1999). Empirical study of particle swarm optimization. In *Proceedings of the 1999 congress on evolutionary computation-CEC99 (Cat. No. 99TH8406)*, volume 3, 1945–1950. IEEE.

Stevens, B.L., Lewis, F.L., and Johnson, E.N. (2015). *Aircraft control and simulation: dynamics, controls design, and autonomous systems*, volume 3. John Wiley & Sons.

Yan Lieven Souza Lúcio, L.S.A. and dos Santos Coelho., L. (2021). Marine predators algorithm approaches on a multivariable fractional PID controller tuning. In C.J.A.B. Filho, H.V. Siqueira, D.D. Ferreira, D.W. Bertol, and R.C.L. ao de Oliveira (eds.), *Anais do 15 Congresso Brasileiro de Inteligência Computacional*, 1–7. SBIC, Joinville, SC.